RESEARCH PAPER

PCCP
www.rsc.org/pccp

Size-selective vibrational spectroscopy of methyl glycolate clusters: comparison with ragout-jet FTIR spectroscopy†

Michal Fárník,[a] Christof Steinbach,[a] Marcus Weimann,[a] Udo Buck,*[a] Nicole Borho[b] and Martin A. Suhm[b]

[a] *Max-Planck Institut für Strömungsforschung, Bunsenstr. 10, D-37073 Göttingen, Germany. E-mail: ubuck@gwdg.de*

[b] *Institut für Physikalische Chemie, Universität Göttingen, Tammannstr. 6, D-37077 Göttingen, Germany*

Received 4th June 2004, Accepted 24th June 2004
First published as an Advance Article on the web 6th July 2004

A comprehensive experimental study of OH-stretching vibrations of size selected methyl glycolate clusters is presented. A depletion spectroscopy experiment in a crossed molecular beam apparatus was employed to scrutinize the cluster size assignment based on pressure dependence studies in a jet-FTIR experiment. First, the dimer to tetramer size assignments of the FTIR spectrum are confirmed by depletion signal angular dependencies measured at the FTIR absorption maxima. Then, independent depletion spectra of the size selected dimers through tetramers are presented. The depletion spectra exhibit peak broadening and blue-shifts with respect to the FTIR spectrum. These differences are discussed and partially explained by cluster heating through energy transfer in the scattering collisions with Ne atoms.

I. Introduction

Selective self-aggregation of biomolecules reflects a subtle interplay of many competing intermolecular interactions such as hydrogen bonds and packing effects. The first step in a reductionist approach to this phenomenon, understanding gas phase aggregation of simple mono-functional molecules such as hydrides and alcohols, has reached a mature state.[1–5]

Complexity increases when two or more different functional groups are present in the aggregating molecules. Stereochemical aspects like chirality and torsional isomerism become important.[6–9] Competition between intra- and intermolecular hydrogen bonds comes into play.[10] Supersonic jet cluster spectroscopy is well suited to map out the onset of this complexity. High resolution spectroscopy can provide ultimate structural information, but it is challenging to apply.[8] UV chromophores allow for conformational selectivity,[7,11,12] but they add substantially to the peripheral complexity of the system. Direct absorption spectroscopy of the vibrational cluster dynamics can supply characteristic fingerprints of hydrogen bond patterns without the need for a UV chromophore.[3,13] Ragout-jet FTIR spectroscopy is a powerful tool to obtain such fingerprints.[14,15] However, it lacks unambiguous cluster size information. Here, we complement the direct absorption approach by a rigorously size-selective spectroscopy technique based on infrared depletion after crossed beam scattering.[16] For the first time, this is demonstrated here for clusters of a multifunctional molecule, methyl glycolate.

Methyl glycolate (MGly) was chosen as a simple prototype system in which OH hydrogen bonds to three types of oxygen atoms can occur (CH_3–O–(C=O)–CH_2–OH). Its gas and condensed phase conformation and vibrational dynamics have already been investigated.[17–19] It is the achiral parent compound of the chiral methyl lactate, for which self-aggregation into homochiral and heterochiral clusters was shown by ragout-jet FTIR spectroscopy to lead to a distinct spectral absorption pattern.[20] Lactate trimers were suggested to prefer homochiral clusters, while tetramers appear to form a distinct heterochiral aggregation pattern. To assist in the cluster size assignment and elucidation of cluster structure and aggregation mechanism, the lactate study has been extended to achiral lactate homologues,[19] such as methyl glycolate and methyl α-hydroxyisobutyrate. Spectroscopic assignment by chemical analogy helped in confirming the cluster size assumption, but it falls short of a rigorous size determination. Stagnation pressure dependence studies[19] are able to provide relative cluster sizes, but no absolute ones, and become difficult to apply whenever the spectral features of various cluster sizes overlap.

This motivates the present study, in which the FTIR-based cluster size assumption for the simple MGly case is scrutinized by size-selected infrared depletion spectroscopy. In this way, pressure scaling arguments can be validated. An extension to the more complex case of methyl lactate will be presented elsewhere.[21]

II. Experiment

A detailed description of the size selective vibrational spectroscopy method and the experimental apparatus employed in the present study can be found elsewhere.[22–24] Briefly, an experiment in crossed molecular beams was employed for cluster size selection. The principle is illustrated pictorially in Fig. 1. The cluster beam is crossed at right angles with the rare gas atom beam, and the clusters are deflected by collisions according to their size: the larger the cluster, the smaller its scattering angle. The largest possible laboratory scattering angle for a given cluster size n, the threshold angle Θ_n, can be calculated based on the Newton diagram.[22] Setting the detector at a laboratory angle Θ between $\Theta_n > \Theta > \Theta_{n+1}$ all the clusters of sizes larger than n are excluded from the detection. Then, setting the detector quadrupole mass analyzer to an appropriate cluster fragment mass larger than M_{n-1}, the smaller clusters can be discriminated from the detection as well. Thus only a signal due to just one cluster size M_n can be recorded.

† Presented at the 3rd Workshop on "Spectroscopy and Dynamics of Molecular Coils and Aggregates" near Kassel, Germany, March 17–20, 2004.

DOI: 10.1039/b408506j

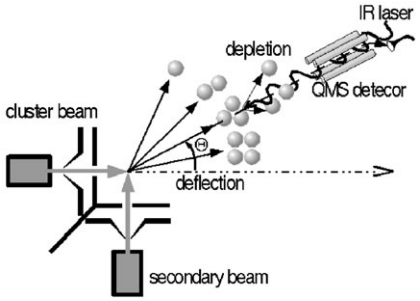

Fig. 1 Schematic principle of the crossed-beam experiment for size selective vibrational spectroscopy of clusters (see text for explanations).

Table 1 Beam parameters of the size selective experiment

	Primary beam	Secondary beam
Nozzle diameter d/μm	90	30
Opening angle 2α/°	30	—
Length l/mm	2	—
Gas	Methyl glycolate/He	Ne
Pressure P_0/bar	1.8	30
Temperature T_0/K	313	303
Concentration c/vol%	0.5	100
Mean velocity $\bar{v}$/m s^{-1}	1670	800
Speed ratio S	26	33

A collimated IR laser beam is directed into the apparatus along the detector axis and overlapped with the size selected cluster beam. If the laser frequency corresponds to a local vibrational mode excitation of the cluster (*e.g.* OH-stretch vibration), the cluster can be excited with the laser pulse. The excitation energy can then be transferred *via* an internal vibrational redistribution (IVR) process and the cluster can eventually break apart. The fragments leave the cluster beam "burning a hole" in the beam by the laser. The "hole" then arrives at the detector with some time delay and spread, resulting in the measured depletion signal at the given laser frequency. The signal is monitored in real-time, using a computer-controlled time-of-flight analyzer triggered by the laser. The laser frequency is scanned resulting in recording the depletion spectrum for clusters of a given size.

The actual experimental setup is described in detail in refs. 25,26. An injection seeded optical parametric oscillator (OPO) generates the infrared radiation, used to excite and dissociate the clusters, in the spectral region from 3000 to 3480 cm^{-1} and from 3510 to 3800 cm^{-1}. It consists of a master oscillator containing a $LiNbO_3$ crystal, which is pumped by the 1064 nm fundamental of a Nd:YAG laser. The tuning is achieved by rotating the crystal and the low-frequency component (idler) is used in the experiment. The master oscillator is seeded by the narrow-bandwidth infrared radiation obtained by difference frequency mixing the output of a pulsed dye laser and the 532 nm second harmonic radiation from the same Nd:YAG laser in a $LiIO_3$ crystal. A typical output energy is ~4 mJ pulse^{-1} with a pulse repetition rate of 20 Hz. The IR radiation bandwidth is ~0.2 cm^{-1}.

In the present study the clusters are produced in a supersonic expansion of methyl glycolate (Acros, 98% purity) in helium buffer gas through a 90 μm conical nozzle. Prior to the expansion the helium passes through a pick up cell containing the liquid methyl glycolate kept at a constant temperature of 313 K in a thermostat bath. The nozzle is heated to the same temperature to prevent its clogging by the condensing gas. The expansion parameters are summarized in Table 1. The cluster beam velocity in Table 1 was measured at the mass of 91 u, which corresponds to the $M \cdot H^+$ ion, *i.e.* the major fragment of the dimer (the larger clusters can possibly contribute to this fragment too). It corresponds to what is expected for seeded beams in the adiabatic limit. For larger protonated fragments up to the protonated tetramer a velocity decrease of up to 3% was observed.

The angular deflection of the clusters was achieved by a Ne atom beam generated in a pinhole expansion (Table 1). The Ne was used since the preliminary measurements with He resulted in depletion signals of the order of only a few percent at maximum. Helium scattering, due to the lower mass of He compared to Ne, results in a lower angular resolution, which may cause the smaller depletion signals, because of the larger overlap of different cluster sizes at a particular scattering angle. In addition, in the atom collisions with the clusters, the cluster internal energy modes can also be excited. The *heated-up* clusters could then break apart more easily upon the additional vibrational excitation with the IR-laser light, resulting in a higher depletion signal. The energy transfer in a collision is, indeed, more efficient with the heavier Ne atoms than with He. We note that the collisional *cluster heating* can also be one of the reasons for differences observed between the size-selected cluster spectra and the expansion cooled jet FTIR spectra, as will be discussed later.

The spectra of size selected clusters are compared with IR spectra obtained with the ragout-jet FTIR apparatus described elsewhere.[14,19] The ragout-jet FTIR-experiment is based on the synchronisation of giant gas pulses (1.3 mol s^{-1}) with rapid acquisition FTIR scans. A Bruker IFS 66v spectrometer equipped with a CaF_2 beamsplitter, 2.5–3.5 μm optical filter, and a 2 mm diameter InSb-detector was employed. A mixture of 0.06% methyl glycolate in He at various stagnation pressures was expanded through a slit nozzle of 120 mm length and 0.4 mm width into a buffer volume of 15 m^3. A series of Roots pumps with a pump capacity of 2000 m^3 h^{-1} allows for repetition rates of 0.03–0.1 Hz.The center of the IR-beam (10 × 20 mm cross-section) is positioned 16 mm downstream the nozzle. Each spectrum (total measuring time ≈20–80 min) results from 100 scans recorded at 2 cm^{-1} resolution.

III. Results and discussion

A. Ragout-jet FTIR-spectroscopy

Fig. 2 shows a sequence of ragout-jet FTIR spectra recorded at different stagnation pressures ($p = 0.3$, 0.4, 0.5, 0.8, 1.0, and 1.2 bar) at a concentration of 0.06% methyl glycolate in He. They agree well with previous spectra of 0.1% methyl glycolate in He given in ref. 19. The plot demonstrates the increase of the OH stretch absorbance of the bands M (3571 cm^{-1}), D_1 (3547 cm^{-1}), D_2 (3512 cm^{-1}), T (3463 cm^{-1}), and Q (3421 cm^{-1}) with pressure. It is found that an increasing red shift relative to the monomer M correlates with a steeper rise of the absorbance. This is quantified by a plot of the relative peak absorbance $A/A_{0.5}$ with respect to the one in the spectrum at 0.5 bar *vs.* the stagnation pressure (Fig. 3). The slope increases in the following order: M (crosses) < D (full and open circles) < T (triangles) < Q (squares). D_1 and D_2 exhibit a similar slope. This leads to the cluster size assignment proposed in ref. 19: D is assigned to dimer, T to trimer and Q to tetramer absorption. The cluster number density N at 1.2 bar can be roughly estimated from the integrated experimental absorbances and approximate band strengths obtained at HF/3-21G level (≈56 km mol^{-1} for M, ≈850 km mol^{-1} for D, ≈2040 km mol^{-1} for T and ≈5700 km mol^{-1} for Q) for selected clusters, *vide infra*. A typical distribution dominated by monomers and monotonically decreasing with cluster size is found in the slit jet expansion.

It has to be stressed that the cluster sizes obtained in this way are not rigorous. Although MGly appears to be a straightforward case up to the tetramer, it is conceivable that conformational isomerism leads to different pressure dependence for a

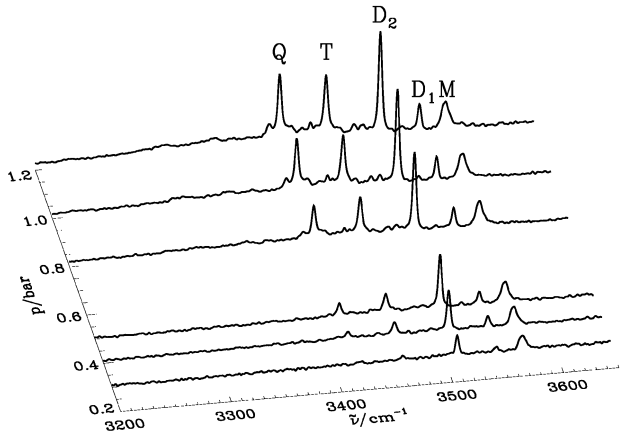

Fig. 2 Ragout-jet FTIR spectra of methyl glycolate expansions (0.06% MGly in He) at different stagnation pressures (p = 0.3, 0.4, 0.5, 0.8, 1.0 and 1.2 bar). The peaks marked M, D_1/D_2, T and Q grow differently with stagnation pressure. The vertical absorbance axis is suppressed for clarity.

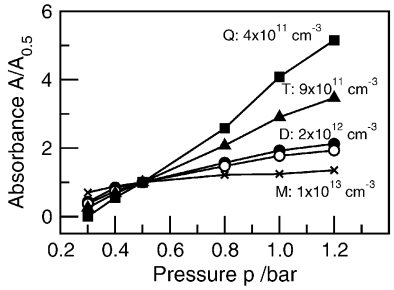

Fig. 3 Cluster size ordering based on the pressure dependence of M (×), D_1 (○), D_2 (●), T (▲) and Q (■) in ragout-jet expansions (see Fig. 2). The ratio $A/A_{0.5}$ of the peak absorbance at stagnation pressure p relative to that at $p = 0.5$ bar is plotted *vs.* pressure p. Steeper slopes correspond to larger clusters. The estimated particle number density (see text) at 1.2 bar is indicated for each cluster size.

given size, and a missing cluster size can also not be ruled out rigorously. Only size-selective vibrational spectroscopy can provide rigorous absolute cluster size assignments, as is outlined below.

B. Size-selective vibrational spectroscopy

Fig. 4 shows the mass spectrum of methyl glycolate clusters measured without the Ne beam scattering in the direction of the primary cluster beam at the laboratory angle $\Theta = 0°$ (with a pinhole inserted into the beam path to prevent detector saturation). The mass spectrum at this geometry simply reflects the cluster beam composition (including the fragmentation upon electron impact ionization) without any size selection. Two surprising features can be noticed in this spectrum: First, the lack of variety of cluster fragments. The spectrum consists almost exclusively of the mass peaks corresponding to the protonated $M_n \cdot H^+$ clusters (M = methyl glycolate molecule) with n = 1,...,4 labelled as dimers (D), trimers (T), tetramers (Q), and pentamers (P), respectively. As outlined in the experimental section, to detect a single cluster size (*e.g.* M_{n+1}) in size selective measurements, a larger deflection angle is chosen to prevent the larger clusters from reaching the detector. To discriminate against the smaller clusters at a given angle, a cluster ion fragment larger than the M_n cluster has to be detected. The mass spectrum in Fig. 4 suggests that the by far dominating such fragment is the $M_n \cdot H^+$ ion. Thus the $M_n \cdot H^+$ mass peaks are used in combination with appropriate deflection angles for detection of the corresponding M_{n+1} clusters in the size selective experiment.

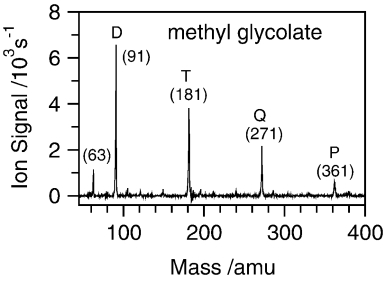

Fig. 4 Mass spectrum of methyl glycolate. The masses (in u) are given in parentheses and the labels suggest the mass peaks used in combination with an appropriate scattering angle for detection of dimer (D), trimer (T), tetramer (Q), and pentamer (P) clusters.

The second surprising feature of the mass spectrum in Fig. 4 is the absence of a strong peak due to the monomer ionization. Only one relatively weak peak appears at the mass of 63 u, which could be a fragment of the ionized monomer. It should be mentioned, that sensitive measurements below 50 u are partly hampered by the larger background, therefore some minor ion signals could have escaped our detection in this region, yet we can definitely exclude any strong contribution. The absence of monomers in our mass spectrum might be surprising in the light of the relatively large monomer contribution in the jet FTIR spectra above, but probably points to differences in the cluster formation and detection in the two experiments. It is difficult to compare the cluster formation efficiency in the two different types of expansions (slit *vs.* conical shaped nozzle), however, it should be noted that it is not only the clustering efficiency, which makes the difference. While in the ragout-jet the entire expansion along a 120 mm long slit is probed with a 10 × 20 mm IR light beam, the cluster beam in the depletion experiment is generated in a 90 μm nozzle, skimmed with a 1 mm diameter skimmer and ionized in the quadrupole mass spectrometer approximately 700 mm downstream from the nozzle. Thus less monomers are expected to arrive to the ionizer region, since (i) they reside at the outskirts of the expansion and are efficiently skimmed, and (ii) the remaining monomers have ample time (>500 μs) to recombine during the flight to the detector generating the clusters. On the contrary, in the ragout jet all the edge regions as well as the early stage regions of the expansion with majority of monomers are probed with the IR light.

The ionization break down pattern of these larger molecular clusters is usually due to fast ion-molecule reactions within the cluster after electron impact ionization.[27,28] The following ionization scenario will probably also occur for the methyl glycolate clusters: upon impact of approximately 100 eV electrons, one of the molecules in the cluster is ionized. It immediately transfers a proton to one of the neighboring molecules, leading to the protonated species $M \cdot H^+$ plus the neutral fragment molecule where the H atom is missing. Similar reactions will occur for the larger species in which the $M \cdot H^+$ ion plays the key role leading to the observed $M_n \cdot H^+$ fragments. This is underlined by the measured mass spectrum which only exhibits protonated ions as reaction products. It is worth mentioning that similar mass spectra, consisting exclusively of protonated clusters with only one relatively small monomer fragment and exceptionally "clean" of any other fragments, could also be obtained for the methyl lactate clusters.[21]

To reveal the extent of cluster fragmentation, a series of time-of-flight (TOF) measurements was done at various deflection angles and various detection masses. An example TOF-spectrum measured at the mass of m = 91 u ($M \cdot H^+$) at the laboratory angle of $\Theta = 5.5°$ is shown in Fig. 5. At the top the actual Newton diagram calculated from the measured beam velocities summarized in Table 1 is illustrated, which indicates

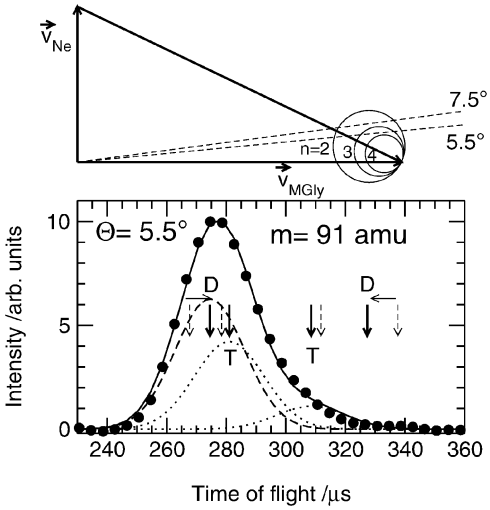

Fig. 5 The Newton diagram (top) for methyl glycolate cluster scattering with Ne atoms. The circles correspond to the appearance of elastically scattered dimers through tetramers (from the largest to the smallest diameter). The graph below shows the TOF distribution measured at $\theta = 5.5^\circ$ and mass $m = 91$ u analyzed for the contribution from dimers (dashed line) and trimers (dotted line). The heavy arrows indicate the peak positions obtained from independent TOF measurements of the dimers and trimers separately. The dashed arrows correspond to the expected peak positions for elastic scattering as indicated in the Newton diagram (top). The light horizontal arrows suggest the shift due to the energy transfer in the collision (see the text for further details).

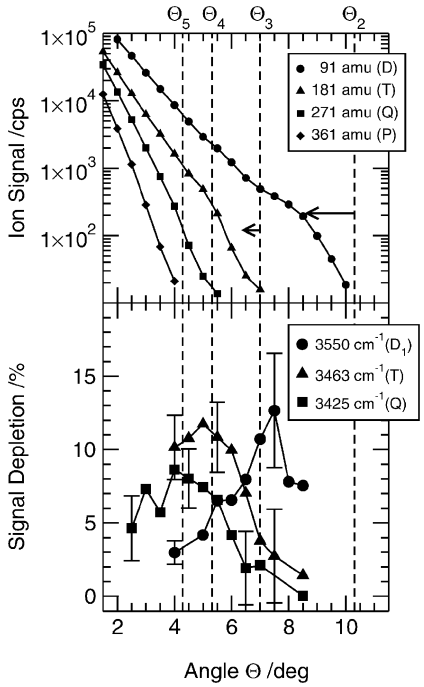

Fig. 6 Angular distributions of methyl glycolate clusters. Ion signal dependencies (top panel) measured for the dimer (D,●), trimer (T,▲), tetramer (Q,■), and pentamer (P,◆) mass peaks (see Fig. 4). The dashed vertical lines denote the threshold scattering angles θ_n for various cluster sizes M_n. The horizontal arrows indicate the threshold angle shifts due to the energy transfer in scattering collisions. The bottom graph shows the depletion measurements for the fixed wavenumbers corresponding to the ragout-jet FTIR spectral peaks (see Fig. 2) assigned to the dimers (D_1,●), trimers (T,▲), and tetramers (Q,■) at a mass of 91 u.

that contributions from both the dimers and trimers should occur at 5.5°. The measured TOF spectrum was analyzed for these contributions (dashed and dotted lines correspond to the dimer and trimer, respectively). The peak positions and widths were determined with independent TOF measurements: (i) at $\Theta = 7.5^\circ$ ($m = 91$ u), where only dimers can be detected, and (ii) at $m = 181$ u ($\Theta = 5.5^\circ$), which corresponds to the trimers only. Therefore, only the relative peak amplitudes were the parameters used in the spectrum fit (full line) in Fig. 5. From this analysis, a ratio of approximately 1:1 was determined between dimer and trimer fragment contributions to the $m =$ 91 u mass peak. This is also in agreement with the angular mass peak dependencies presented below.

In addition, the actual TOF peak positions (indicated by the heavy arrows in Fig. 5) are shifted with respect to their positions expected from elastic collisions (dashed arrows), which indicates some energy transfer from Ne atoms to the internal excitation of the clusters in the collisions. This energy transfer could be quantified by $\Delta E/E \approx 0.37$ and 0.15 for dimers and trimers, respectively (for even larger clusters the energy transfer was more difficult to quantify precisely at the present experimental resolution). This result can be qualitatively understood, since the Ne atom can apply a larger torque to the more structured and floppier dimers than to the heavier and more compact larger clusters (see cluster structures below and in ref. 19).

The angular dependence of the individual $M_n \cdot H^+$ peaks shown in the top panel of Fig. 6 also points to the cluster fragmentation pattern and collisional energy transfer. The vertical dashed lines in Fig. 6 mark the positions of the threshold scattering angles for dimers (Θ_2), trimers (Θ_3), tetramers (Θ_4), and pentamers (Θ_5), as obtained from the Newton diagram assuming elastic scattering. It is noticed that the measured angular dependences fall off somewhat before the corresponding threshold angles. This is, indeed, due to the above mentioned energy transfer in the collisions. The horizontal arrows indicate the shift in the threshold angle assuming an inelastic collision with the energy transfer $\Delta E/E \approx 0.37$ and 0.15, as obtained above from the TOF measurements for the dimers and trimers, respectively. This shift is in good agreement with the corresponding fall-off of the measured angular distribution. In the angular distribution at $m = 91$ u (circles), a second slight stepwise increase can be noticed at around $\Theta = 6^\circ$, which is an indication for the trimer fragment contribution at this mass, as was also revealed by the TOF measurements.

In the first spectroscopic experiment we tried to confirm the cluster size assignment of the most pronounced lines measured in the ragout-jet FTIR experiment.[19] For that purpose the laser was tuned to these frequencies and the laser induced depletion signal was measured as a function of the laboratory deflection angle Θ in the scattering arrangement. Since these signals are independent of the mass, we used the smallest cluster fragment mass $M \cdot H^+$ for their detection. The results are shown in the lower panel of Fig. 6. The selected wavenumbers, listed in the figure, correspond to the jet FTIR spectral peaks shown in Fig. 2. The depletion signals of a particular cluster size n as well as the angular distributions of the corresponding ion fragment signals are supposed to exhibit a steep fall-off at the corresponding threshold angle. This is apparently the case for the trimer (triangles) in Fig. 6: both the ion signal (top) and the depletion signal at 3463 cm^{-1} (bottom) fall off close to the trimer threshold angle Θ_3, corrected for the energy transfer to $\approx 6.4^\circ$. This confirms the assignment of this peak (T) in the FTIR spectrum to the trimer.

The corrected threshold angle for the dimer is $\approx 8.6^\circ$ as is confirmed by the ion signal angular distribution (full circles, top panel). The depletion signal at 3550 cm^{-1} (full circles, lower panel) falls off at somewhat smaller angles but, on the other hand, it still keeps increasing beyond Θ_3, leaving the only possibility to interpret this peak (D_1) as being due to the dimer. A monomer contribution is ruled out, as these depletion measurements were performed at 91 u. The dimer threshold angle Θ_2 could not quite be reached in the depletion

measurements due to the strong fall-off of the corresponding ion signal, which is also the reason for the error bars gradually increasing with the scattering angle. Although the D_1 and T absorption peak assignments to the dimer and trimer, respectively, could be readily confirmed, the depletion for the absorption peak Q at 3425 cm^{-1} (squares), assigned to the tetramer, falls off somewhat beyond the corresponding Q ion signal (top panel), overshooting also the corresponding threshold angle $\Theta_4 = 5.1°$. Yet, there is a distinct shift in this depletion fall-off to smaller scattering angles compared to the trimer depletion (triangles), which supports the tetramer assignment. This shift remains even if both the trimer and the tetramer depletion signals are scaled to the same maximum value. This conclusion is also supported by the size selected depletion spectra discussed later.

It is worth noting that the depletion signal of a particular cluster size also decreases towards smaller scattering angles. This is due to the increasing contribution from larger clusters in the ion signal, which are scattered into smaller angles, and which do not predissociate at the particular laser frequency. If the larger clusters also absorb at this frequency another stepwise increase in the depletion signal may occur at the corresponding threshold angle (similar to the second stepwise increase noticeable in the 91 u ion signal due to the trimer fragments discussed above). Nevertheless, if the relative depletion is small, the stepwise increase is usually overruled by the strong exponential increase of the total ion signal, so that such a contribution is difficult to recognize.

The final step is the direct measurement of the complete vibrational spectrum of the size selected MGly complexes as described in the experimental section. The results are shown in Fig. 7. At the top panel the corresponding ragout-jet FTIR spectrum of a methyl glycolate/He expansion (0.8 bar, $\approx$0.06%) is shown. The size selected spectra correspond to dimers, trimers and tetramers, from top to bottom. The corresponding scattering angles and detection ion masses are outlined in the figure. The detection mass for an *n*-mer was always that of the $M_{n-1} \cdot H^+$ ion fragment to discriminate against smaller clusters. The scattering angle was in all cases somewhat smaller than the corresponding threshold angle to obtain a higher ion intensity (see the top panel in Fig. 6). We note that the shaded area cannot be reached in the experiment because of the intensity gap of the OPO. In spite of the large error bars, caused by the small ion signals, the following conclusions can be drawn from these spectra:

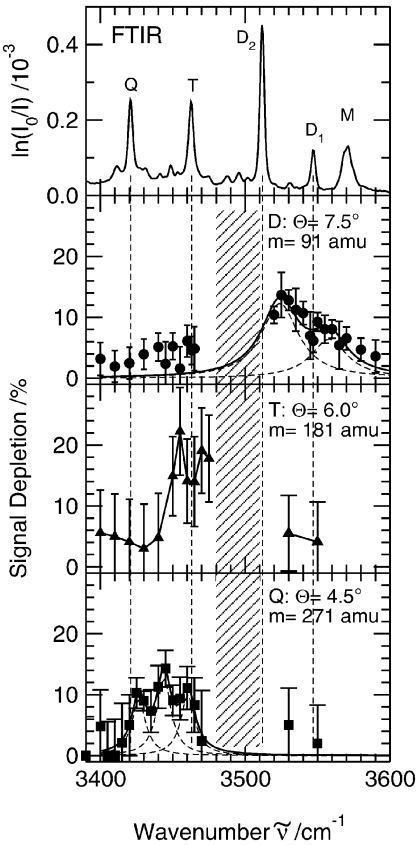

Fig. 7 The top panel shows the ragout-jet FTIR spectrum at 0.8 bar (0.06% MGly in He) from Fig. 2 for comparison. Below are the vibrational depletion spectra of methyl glycolate clusters M_n of various sizes $n = 2$, 3 and 4 (from top to bottom). The laboratory scattering angle and the detection mass are indicated at each spectrum.

(i) Generally, the measurements confirm the FTIR spectral assignments. The dimers apparently absorb mostly in the region above 3500 cm^{-1} (where the D_1 and D_2 peaks occur), the trimer absorption starts to occur at 3450 cm^{-1} close to the T peak, and the tetramers apparently exhibit a broad distribution between 3420 cm^{-1} and 3470 cm^{-1} close to but slightly shifted from the Q peak.

(ii) On the other hand, differences can be observed between the depletion and the jet spectra: the depletion spectra features are significantly broader than the jet absorption peaks, and they do not peak exactly at the jet maxima positions. In fact, the dimer (D_1 and D_2) and the tetramer (Q) are shifted to the blue by approximately 11 cm^{-1}, 12 cm^{-1} and 23 cm^{-1}, respectively, while the trimer (T) shift is difficult to quantify due to the OPO intensity gap. The reason for the larger bandwidth and the shift of the depletion spectra features is very probably the cluster heating in the collisions with the rare gas atoms, already mentioned in the experimental section.

It has been determined by the TOF analysis that about 37% and 15% of the relative collision energy with the Ne atoms ($\sim$70 meV) is transferred to the dimers and trimers, respectively. This means that 26 meV are deposited into internal cluster excitation of the dimer and 10 meV into that of the trimer. In a previous investigation of methanol dimers a linear correlation of the energy transfer ΔE and the overall bandwidth Γ was observed within a variation of more than a factor of ten.[29] The estimated width of the measured distributions of $\Gamma = 30$ cm^{-1} for the two dimer peaks of the present experiment of the much larger methyl glycolate fits very well into that scheme. If we take the proportionality of ΔE and Γ for granted, we can estimate the trimer width to be about 15 cm^{-1} based on the measured energy transfer $\Delta E = 10$ meV. Probably the main peak of the trimer is shifted into the intensity gap of the OPO so that a direct comparison is not possible. The fitted width of the tetramer bands is with 12 cm^{-1} a bit smaller and thus, according to the correlation caused by an energy transfer of about 8 meV. The underlying mechanism of the broadening is apparently inhomogeneous. With increasing energy transfer ΔE more and more internal vibrational states are excited and can be coupled effectively to the hydrogen bond break down upon the initial laser excitation. In addition, these low frequency excitations have each a different OH-stretch frequency, depending on how much its excitation weakens the hydrogen bond. Therefore the final spectrum is a superposition of hot bands from the most red-shifted cold transition back to the monomer value.

These considerations lead us to the discussion of the blue shift of the depletion spectra with respect to the FTIR spectra which increases from 11 and 12 cm^{-1} of the dimer to 23 cm^{-1} of the tetramer. The main reason is, as was already mentioned, the weakening of the hydrogen bond by the internal excitation of the cluster. However, it is difficult to estimate quantitatively the expected blue shift dependence on the cluster size, because several effects have to be considered, which can partly point in opposite directions: (i) Since the intermolecular hydrogen bond strength increases with the cluster size, larger clusters are expected to be shifted more with *cluster heating*. (ii) However, the energy deposited into the trimers in the collision is less (by a

factor of about 2.5) than the 26 meV deposited into the dimers, which tends to make the expected temperature of the trimers and thus the corresponding shift smaller. (iii) In addition, the number of degrees of freedom, over which the deposited energy can be distributed, increases modestly (depending on the modes considered) with the cluster size, which also tends to lower temperatures and thus smaller shifts.

We tried to estimate the blue-shift by extrapolating the measured shift of the monomer as function of the temperature and by calculating the temperature resulting from the energy transfer. For example the heating from 20 K to 300 K results in a blue shift of $\approx 10\%$ in the O–H stretching vibration of the monomeric α-hydroxy carbonyl compounds, due to the internal hydrogen bond softening.[20] Then the clusters should be shifted by 3 to 20 cm^{-1} at about 300 K. But this temperature is not reached in the experiment. For the dimer the energy transfer $\Delta E = 26$ meV leads to a temperature of about 50 K estimated from the structure simulations and the calculated frequency distributions using the partition functions for thermodynamic properties in equilibrium conditions. If we restrict excitation to rotation only, a temperature of ≈ 200 K results, but the hot band blue shift is lost. Apparently, the shift is amplified in the nonlinear depletion spectra due to preferential dissociation of excited clusters.

The relative intensities of the different depletion spectra for the different cluster sizes cannot be compared with the relative absorption peak heights in the jet FTIR spectrum. While the latter are a measure of the relative cluster size populations (multiplied by the IR transition probabilities for the individual cluster sizes and structures), the former reflect a complicated product of the excitation probability and the relative decay probabilities of the various cluster sizes. Nevertheless, there are some resemblances in the band shapes. For the tetramer, the three peaks of the depletion spectrum can also be found in the ragout jet spectrum, if we interpret the small satellites to the left and right of the main peak as separate bands. Similar considerations hold for the trimer with one satellite to the left of the main peak which is shifted into the intensity gap.

We note that an interesting correlation has been observed in the literature between the frequency shift and the width of the OH stretch frequency bands of hydrogen bonded systems.[30–32] Based on the consideration that both effects should be driven by the same matrix elements the width Γ should be proportional the square of the shift $(\delta\omega)^2$. The correlation is not at all fulfilled by the present data. This is another evidence that the line width is not homogeneously broadened for these large systems, a fact that has already been suggested in a previous analysis.[31]

Our exploratory quantum chemical calculations on clusters of α-hydroxy-carbonyl compounds, ranging from HF/3-21G to MP2/6-31+G* level, indicate two types of dimer structures, in close analogy to the glycidol case.[13] Eight-ring conformers with two O–H···O=C bonds and five-ring conformers with an O–H···O–H···O=C arrangement compete with each other. The spectrum is consistent with either a mix of two conformers or with a single five-ring conformer exhibiting two IR active OH stretch vibrations. For the trimer, a ring structure with threefold symmetry bound by OH···OH hydrogen bonds with some OH···O=C character is predicted at most levels of theory, with all molecular backbones being on one side of the hydrogen-bonded ring (see Fig. 8, top). This is consistent with a single dominant trimer IR absorption which is found in the experiments. For the tetramer, various structures with twofold or fourfold (see Fig. 8, bottom) symmetry were located on the potential energy hypersurface, giving rise to one or two strong IR transitions similar to the case of methanol tetramers.[26,33,34] Here, the lowest energy isomer with S_4 symmetry and the arrangement of the CH_3 groups up-down-up-down exhibits one strong band with a weak satellite, while the next isomer with lower energy and symmetry with the CH_3 arrangement

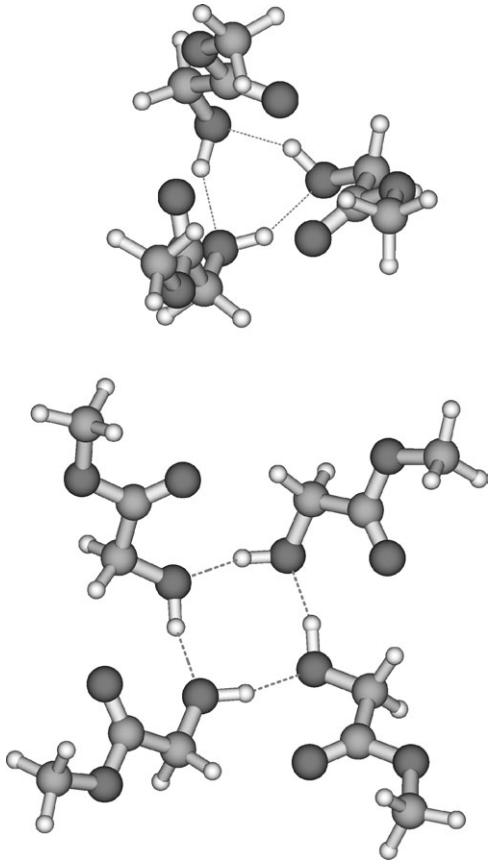

Fig. 8 Symmetric structures of methyl glycolate trimer and tetramer.

up–up–down–down shows two bands of equal intensity. Apparently, the single main peak of the MGly-tetramer in the experiments is an indication of a more symmetric structure as was found for the trimer. There is the possibility that the two satellite peaks are an indication of a second more asymmetric isomer.

A systematic quantum chemical analysis of this conformational problem is beyond the scope of the present contribution, but a subtle energetical detail should be mentioned: In contrast to alcohol clusters, where the tetramer typically has the largest stepwise dissociation energy,[4] it appears to be the trimer which is most stable with respect to evaporation of a monomer in α-hydroxy-carbonyl compounds. The carbonyl groups can stabilize the strained trimer OH···OH hydrogen bonds particularly well by secondary coordination to both OH and CH groups (Fig. 8). Nevertheless, the dissociation energies of α-hydroxy-carbonyl clusters are found to be comparable in magnitude to those of simple alcohol clusters, because the additional interaction of the carbonyl group is partially present in the monomeric dissociation products as well. OH-stretch excitation is therefore expected to be close to or even below the dissociation threshold for some of the cluster sizes.

IV. Conclusions

In this contribution we have applied scattering from atomic beams in order to get information on the cluster sizes involved in previous FTIR absorption experiments. In a first series of investigations angular distributions of depletion signals for several selected IR wavenumbers were measured in order to assign them to their corresponding cluster sizes. The results essentially confirm the FTIR assignment: (i) the D_1 absorption at 3550 cm^{-1} is due to the dimers; (ii) at 3463 cm^{-1} (T) trimers absorb, and finally (iii) the peak Q at 3425 cm^{-1} corresponds to tetramer absorption. We note that a depletion signal fall-off at a particular threshold angle determines mainly the smallest

contributing cluster size. Also the angular distance between the various threshold angles gradually decreases with the cluster size and therefore the resolution of larger cluster sizes becomes difficult. Thus this method is best suited for analyzing a number of separated lines originating from different clusters.

In a second series of experiments, we have measured the IR depletion spectra for completely size selected methyl gycolate dimers, trimers, and tetramers. The size selected spectra agree well with the general range of frequencies of the ragout-jet FTIR ones (see Fig. 7). They differ, however, in their shape, bandwidth, and maximum peak positions. The main reason for this behaviour is the higher temperature of the clusters caused by the collisional heating during the deflection and the preferential dissociation of excited rotational and intermolecular vibrational levels. This leads, in turn, to much broader features in the observed spectra. In addition, a blue-shift of the peak maxima is observed which is due to the hydrogen bond weakening in the heated clusters. The range of the peak broadening is consistent with a correlation with the amount of energy transferred in the deflection collisions, found previously for methanol dimers.[29] The underlying mechanism is inhomogeneous broadening caused by the excited intermolecular vibrational levels. The blue shift of the photodepletion data with respect to the ragout-jet FTIR results, which increases with increasing cluster size, is caused by the weakening of the hydrogen bond by the internally excited states. It is, as expected, roughly proportional to the red shift of the main cluster bands with respect to the monomer.

For the dimer the conclusions are the same as those obtained previously. For the trimer the calculations support a very stable ring configuration of O–H···O–H hydrogen bonds with all three rest groups pointing into the same direction in agreement with the single peak in the ragout-jet FTIR spectrum. The dominant tetramer peak also suggests a symmetric structure, but the weak satellites as well as exploratory calculations do not rule out more complex conformations with reduced symmetry.

Acknowledgements

Support by the Deutsche Forschungsgemeinschaft *via* SFB 357 and GRK 782 is gratefully acknowledged. We thank A. Bochenkova, C. Emmeluth and U. Schmitt for help and discussions.

References

1 L. Oudejans and R. E. Miller, *J. Chem. Phys.*, 2000, **113**, 971–978.
2 U. Buck and F. Huisken, *Chem. Rev.*, 2000, **100**(11), 3863–3890.
3 R. A. Provencal, R. N. Casaes, K. Roth, J. B. Paul, C. N. Chapo, R. J. Saykally, G. S. Tschumper and H. F. Schaefer III, *J. Phys. Chem. A*, 2000, **104**, 1423–1429.
4 D. Zimmermann, T. Häber, H. Schaal and M. A. Suhm, *Mol. Phys.*, 2001, **99**, 413–426.
5 M. Losada and S. Leutwyler, *J. Chem. Phys.*, 2002, **117**, 2003–2016.
6 T. A. Beu, U. Buck, M. Ettischer, I. Hobein, J. G. Siebers and R. Wheatley, *J. Chem. Phys.*, 1997, **106**, 6806–6812.
7 N. Seurre, J. Sepioł, K. Le Barbu-Debus, F. Lahmani and A. Zehnacker-Rentien, *Phys. Chem. Chem. Phys.*, 2004, **6**, 2867–2877.
8 A. K. King and B. Howard, *Chem. Phys. Lett.*, 2001, **348**, 343–349.
9 H. Schaal, T. Häber and M. A. Suhm, *J. Phys. Chem. A*, 2000, **104**, 265–274.
10 M. J. Tubergen, C. R. Torok and R. J. Lavrich, *J. Chem. Phys.*, 2003, **119**, 8397–8403.
11 D. Spangenberg, P. Imhof, W. Roth, C. Janzen and K. Kleinermanns, *J. Phys. Chem. A*, 1999, **103**, 5918–5924.
12 R. Wu, P. Nachtigall and B. Brutschy, *Phys. Chem. Chem. Phys.*, 2004, **6**, 515–521.
13 N. Borho and M. A. Suhm, *Phys. Chem. Chem. Phys.*, 2002, **4**, 2721.
14 T. Häber, U. Schmitt and M. A. Suhm, *Phys. Chem. Chem. Phys.*, 1999, **1**, 5573–5582.
15 T. Häber, U. Schmitt, C. Emmeluth and M. A. Suhm, *Faraday Discuss.*, 2001, **118**, 331–359.
16 U. Buck and H. Meyer, *Phys. Rev. Lett.*, 1984, **52**, 109.
17 S. Jarmelo and R. Fausto, *J. Mol. Struct.*, 1999, **509**, 183–199.
18 S. Jarmelo, T. M. R. Maria, L. P. Leitão and R. Fausto, *Phys. Chem. Chem. Phys.*, 2000, **2**, 1155–1163.
19 N. Borho and M. A. Suhm, *Phys. Chem. Chem. Phys.*, 2004, **6**, 2885.
20 N. Borho and M. A. Suhm, *Org. Biomol. Chem.*, 2003, **1**, 4351.
21 M. Fárník, C. Steinbach, M. Weimann, N. Borho, M. A. Suhm and U. Buck, unpublished results, 2004.
22 U. Buck and H. Meyer, *J. Chem. Phys.*, 1986, **84**, 4854.
23 U. Buck, *J. Phys. Chem.*, 1994, **98**, 5190.
24 U. Buck, *Adv. At. Mol. Opt. Phys.*, 1995, **35**, 121.
25 U. Buck, X. J. Gu, C. Lauenstein and A. Rudolph, *J. Chem. Phys.*, 1990, **92**, 6017.
26 U. Buck and I. Ettischer, *J. Chem. Phys.*, 1998, **108**, 33.
27 U. Buck and C. Lauenstein, *J. Chem. Phys.*, 1990, **92**, 4250.
28 U. Buck, *J. Phys. Chem.*, 1988, **92**, 1023.
29 U. Buck, C. Lauenstein and A. Rudolph, *Z. Phys. D*, 1991, **18**, 181.
30 R. E. Miller, *Science*, 1988, **240**, 447.
31 R. LeRoy, M. R. Davies and M. E. Lam, *J. Phys. Chem.*, 1991, **95**, 2167.
32 R. Rey, K. B. Møller and J. T. Hynes, *Chem. Rev.*, 2004, **104**, 1915.
33 U. Buck, J. G. Siebers and R. J. Wheatley, *J. Chem. Phys.*, 1998, **108**, 20.
34 M. V. Vener and J. Sauer, *J. Chem. Phys.*, 2001, **114**, 2623.

